Development of a Simulation Tool for the Cornering Performance Analysis of 6WD/6WS Vehicles

Kunsoo Huh*, Kyungyoung Jhang*, Jaeeung Oh, Joonyoung Kim*** and Jaehee Hong*****

(*Received December 27, 1997*)

In this study, a simulation tool is developed to investigate non steady-state cornering performance of 6WD/6WS special-purpose vehicles. 6WD vehicles are believed to have good performance in off-the-road maneuvering and to have fail-safe capabilities. But the cornering performance of 6WS vehicles are not yet well understood in the relevant literature. In this paper, 6WD/6WS vehicles are modeled as an 18 DOF system that considers non-linear vehicle dynamics, tire models, and kinematic effects. The vehicle model is constructed as a simulation tool using MATLAB/SIMULINK so that input/output and vehicle parameters can be changed easily with the modulated approach. Cornering performance of 6WS vehicles is analyzed for brake steering and pivoting, respectively. Simulation results show that cornering performance depends on the middle-wheel steering as well as front/rear wheel steering. In addition, a new 6WS control law is proposed in order to minimize the sideslip angle. Lane change simulation results demonstrate the advantage of 6WS vehicles with the proposed control law.

Key Words: 6WD, 6WS, Non Steady-State, Off-the-Road, Pivoting, Sideslip Angle, Lane Change

Nomenclature

Subscript i	: i-th wheel
V_x	: Forward velocity
V_y	: Lateral velocity
V_z	: Vertical velocity
V	: Vehicle speed
Φ	: Roll angle
θ	: Pitch angle
F_{yi}	: Side force
F_{zi}	: Vertical load
F_{yf}	: Lateral force of the front wheel
F_{ym}	: Lateral force of the middle wheel
F_{yr}	: Lateral force of the rear wheel
C_f	: Front cornering stiffness
C_m	: Middle cornering stiffness
Ψ	: Yaw angle
p	: Roll rate
q	: Pitch rate
r	: Yaw rate
I_x, I_y, I_z	: Principle centroid moment of inertia
I_{wi}	: Rotating wheel inertia
F_{xi}	: Tractive force
R_i	: Rolling resistance
s_i	: Longitudinal slip
α_i	: Slip angle
r_{wi}	: Tire radius
μ_i	: Friction coefficient
ε_r	: Adhesion reduction coefficient
h	: Height of c. g. above ground
C_r	: Rear cornering stiffness
δ_i	: Steer angle
ω_i	: Axle rotational speed
T_i	: Drive torque
β	: Sideslip angle

* Dept. of Precision Mechanical Engineering, Hanyang Univ.
** Dept. of Automotive Engineering, Hanyang Univ.
*** Graduate Student, Dept. of Precision Mechanical Engineering, Hanyang Univ.
**** Research Engineer, KIA Motors, R&D Center

σ : Suspension deflection
z_t : Unsprung mass vertical situation
z_{rl} : Road-input of the wheel

1. Introduction

Multi-wheel drive vehicles applied to special environments are believed to have more tractive force, better steerability and stability. Some of the vehicles have middle wheels under the center section of the hull and are named 6WD/6WS (6-wheel-drive/6-wheel-steering) vehicles. These 6WD/6WS vehicles are known to have sufficient structural stability because of the load distribution, and thus minimize the tendency of pitching during abrupt braking or acceleration. Because 6WD vehicles typically possess better traction and braking capability than 2WD or 4WD vehicles, they can accelerate or brake better off-the-road and they can continue to move when one or two of their tires are blown or there are transverse rigid-type obstacles. However, the cornering performance of 6WS (6-wheel-steering) vehicles, which are believed to have better maneuverability than 2WS or 4WS vehicles, is not yet well understood in the relevant literature. Although 4WS vehicles have been extensively studied and their results can be extended to 6WS vehicles, few results are reported cornering six wheel steering coordination.

In this paper, six wheel steerings coordination is investigated for cornering performance analysis. 6WD/6WS vehicles are modeled as an 18 DOF system which includes 12 DOF nonlinear vehicle dynamics, 6 DOF wheel dynamics, tire model and kinematic effects. This model is constructed into a simulation tool using MATLAB/SIMULINK and its cornering performance is evaluated under various steering conditions. Simulations are executed for cornering combined with braking and pivoting, respectively. In order to minimize the sideslip angle during lane changes, a new 6WS control law is proposed and its results are compared to conventional 4WS control laws.

2. Background

Research on vehicle dynamics and simulations has increased enormously, from simulation of high-order models with all types of non-linearities to simulation and control of linear bicycle models. Smith and Starkey (1995) studied the relationship between model complexity and simulation accuracy with three different vehicle models and concluded that linear models are not suitable at high g's maneuvering. Nalecz and Bindermann (1988) utilized a 3 DOF model including suspension and steering systems, and demonstrated that roll steer and lateral weight transfer were crucial factors in cornering performance. Xia and Law (1992) compared various 4WS control algorithms based on a nonlinear 8 DOF model with kinematic effects. Abe (1989) proposed a 4WS control law in order to minimize the sideslip angle using a linear 2 DOF model.

Tire models which are essential for vehicle dynamics study have been actively investigated. Examples of the proposed models are theoretical models based on the friction ellipse and empirical models based on experimental data.

In commercial vehicle research, characteristics of heavy vehicles are different from passenger vehicles because of the increased weight and number of wheels. Pillar and Braun (1995) implemented various steering algorithms on multi-wheeled heavy trucks. Das et al. (1993) derived a dynamic model of heavy trucks and executed simulations to study stability and maneuvering. Hata et al. (1992) experimented with medium-duty trucks with 4WS and investigated their controllability and stability.

Studies on 6-wheeled vehicles have concentrated on armored vehicles because they are favored by military operations. Examples of 6-wheeled armored vehicles are: M38, made in the U. S. A, Alvis Saladin of Britain; and Gendron Somua of France. These 6-wheeled vehicles adopted independent suspensions and all-wheel-drive systems in order to have comparable off-the-road performance as tracked vehicles. The implemented prototypes are reported to have

Table Vehicle parameters

Vehicle mass	M	5000 kg
Unsprung mass	m	190 kg
Moment of inertia (X Axis)	I_x	3619.5 kgm^2
Moment of inertia (Y Axis)	I_y	12306.5 kgm^2
Moment of inertia (Z Axis)	I_z	14478 kgm^2
Distance from c.g. to front axle	l_f	1.8 m
Distance from c.g. to middle axle	l_m	0.2 m
Distance from c.g. to rear axle	l_r	2.2 m
Distance from c.g. to round	h	1.25 m
Track width	2d	3 m
Spring coefficient of suspension	k	89266 n/m
Damping coefficient of suspension	b	1762.5 Ns/m
Spring coefficient of the tire	K_t	682960 N/m
Roll bar stiffness	K_r	2566 Nm/rad
Rotating wheel inertia	I_ω	6.25 kgm^2
Tire radius	r_w	0.5 m
Nominal longitudinal stiffness	C_s	168118 N/skid
Nominal cornering stiffness	C_α	112078 N/rad
Friction coefficient	μ	0.6
Road adhesion reduction factor	ε_r	0.015 s/m
Front roll steer coefficient	K_{rsf}	0.15
Middle roll steer coefficient	K_{rsm}	0.15
Rear roll steer coefficient	K_{rsr}	0.15
Lateral force lag time coefficient	C_{tl}	1
Ratio of camber angle to roll angle	K_γ	0.1

adequate off-the-road performance except on clay soil, and they were also able to pivot like tracked vehicles.

3. 6WD/6WS Vehicle Model

The 6WD/6WS vehicle considered in this paper consists of six 30 hp electric motors, electrically controlled steering, and 5 ton weight. It has a sprung mass and six unsprung masses and independent suspensions. The detailed description of the vehicle is listed in Table. The dynamic characteristics of the vehicle are modeled based on the following assumptions:

- Longitudinal, lateral, vertical, rolling, pitching, and yawing motion are considered.
- Vertical motion of the unsprung mass is identical to the z-direction of the vehicle-fixed axis.
- Vertical motion of the sprung mass is transfered through the suspension.
- The longitudinal and the lateral load transfer is considered.
- Kinematic effects such as roll steer, camber angle and tire side force lag are considered.

Vehicle Dynamics Model - Figure 1 shows a body-fixed coordinate system of the 6-wheeled vehicle. Figure 2 shows the suspension linked with each tire. A side view of the wheel rotation model is shown in Fig. 3, the variables are explained in the Nomenclature and Table.

Based on the above assumptions and coordinates, the vehicle is modeled as the following 18 DOF system:

longitudinal motion: $M\cdot(\dot{V}_x+V_z\cdot q-V_y\cdot r)=F_x$ (1)

lateral motion: $M\cdot(\dot{V}_y+V_x\cdot r-V_z\cdot p)=F_y$ (2)

vertical motion: $M\cdot(\dot{V}_z+V_y\cdot p-V_x\cdot q)=F_z$ (3)

rolling motion: $I_x\cdot\dot{p}+(I_z-I_y)\cdot q\cdot r=M_x$ (4)

pitching motion: $I_y\cdot\dot{q}+(I_x-I_z)\cdot r\cdot p=M_y$ (5)

yawing motion: $I_z\cdot\dot{r}+(I_y-I_x)\cdot p\cdot q=M_z$ (6)

unsprung mass motion: $m_i\cdot\ddot{z}_i=-F_{si}+K_{ti}\cdot(z_{ri}-z_i)+(-1)^{i+1}\frac{K_{ri}\cdot\phi}{2d}$, $(i=1\sim6)$ (7)

wheel rotation: $\dot{\omega}_i=\frac{1}{I_{wi}}\cdot(T_i-r_{wi}\cdot F_{xi}+r_{wi}\cdot R_i)$ (8)

where Fx and Fy are resultant forces about the x-axis and y-axis, respectively. These forces are expressed as the tire force, rolling resistance and aerodynamic drag. Fz is expressed as the resultant force of the road input of the tire and suspension force denoted Fs. Mx, My, and Mz are resultant moments about the x-axis, y-axis, and z-axis, respectively. Expressions for these variable are omitted for simplicity.

Tire Model - Because vehicle tires generate traction and lateral force when in contact with the

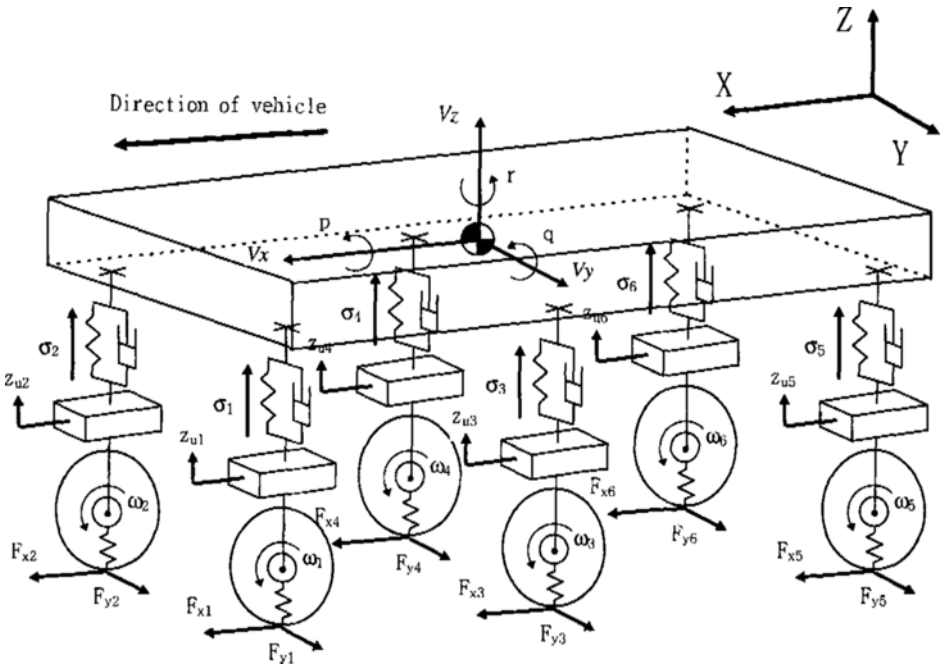

Fig. 1 Body-fixed coordinate system

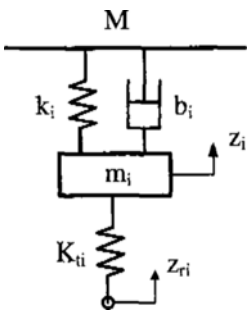

Fig. 2 Suspension system

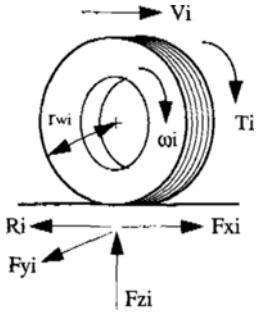

Fig. 3 Wheel rotation

terrain, they are the most difficult components for vehicle modeling along with nonlinearities. In this study, Dugoff's model, where tire forces are expressed as the slip angle and the slip ratio, is introduced. The longitudinal and the lateral forces at the i-th wheel are expressed as

$$F_{xi}=\frac{C_s\cdot s_i}{1-s_i}\cdot X_i\cdot(2-X_i) \tag{9}$$

$$F_{yi}=\frac{C_\alpha\cdot \tan\alpha_i}{1-s_i}\cdot X_i\cdot(2-X_i) \tag{10}$$

$$s_i=\begin{cases}\dfrac{r_w\omega_i-V_i}{r_w\omega_i} & \text{if } r_w\omega_i\le V_i \text{ (in acceleration)}\\[2ex] \dfrac{V_i-r_w\omega_i}{V_i} & \text{if } r_w\omega_i>V_i \text{ (in braking)}\end{cases} \tag{11}$$

$$X_i=\begin{cases}X_i & \text{if } X_i\le 1\\ 1 & \text{if } X_i>1\end{cases} \tag{12}$$

$$X_i=\frac{\mu_i\cdot F_{zi}\cdot(1-s_i)\cdot(1-\varepsilon_r\cdot V_i\cdot\sqrt{s_i^2+\tan^2\alpha_i})}{2\sqrt{C_s^2\cdot s_i^2+C_\alpha^2\cdot\tan^2\alpha_i}} \tag{13}$$

where Xi denotes the non-dimensional total slip coefficient considering the slip angle and the slip ratio. It becomes 1 when there is no sliding between the tires and the road. In order to minimize the sliding of the tires, it is necessary to keep the value of Xi large. If sliding occurs excessively, the value of Xi approaches zero and the tire force becomes very small. Fzi is the vertical force considering the longitudinal and the lateral weight transfer.

Kinematic Effects

(1) Roll Steer : Roll steer is defined as the additional steering of the front or rear wheels due to the rolling of the sprung mass. Generally, roll steer is known to complicately affect the handling response from the steering input, but in this study

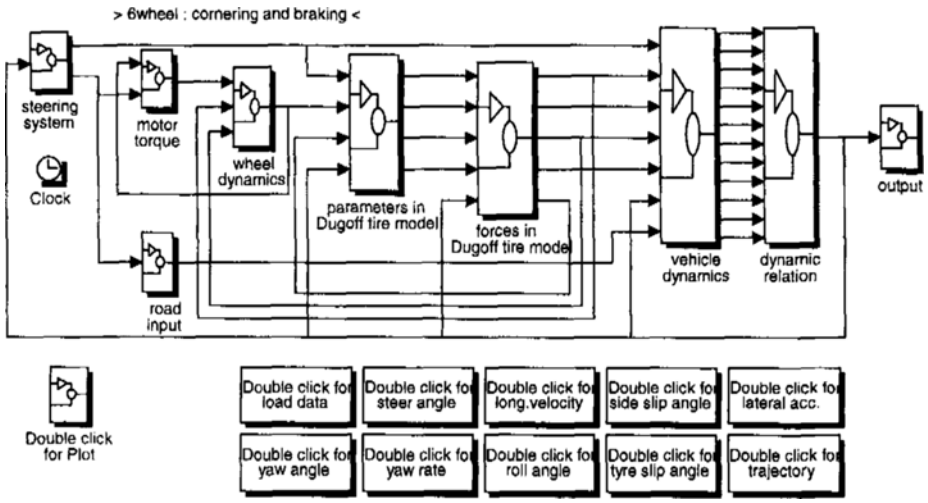

Fig. 4 Simulink model

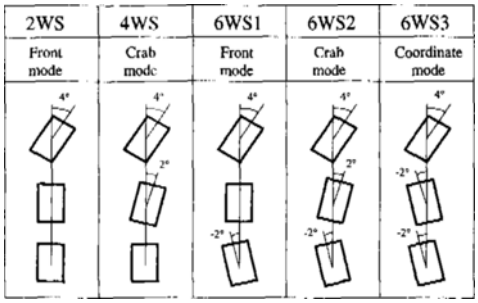

Fig. 5 Five different steering modes

this effect is modeled as a linear function of the roll angle.

(2) Tire Side-Force Lag : There is a time lag at the tires between the steering input and the lateral force generation. In other words, the tires must roll through some distance in order to develop a slip angle and to generate the lateral force. In this study this time lag is modeled as a first-order dynamic system with a time delay.

(3) Camber Angle : Camber on a wheel produces a lateral force known as the camber thrust, and this force allows the vehicle to be understeered. The camber thrust is assumed to be a linear function of the camber angle in this study.

4. Simulation Tool

The 6WD/6WS vehicle model derived in the previous section is constructed into a simulation tool using MATLAB/SIMULINK. Figure 4 shows a simulink model of the overall system and each block is composed of hierarchical sub-blocks. For the convenience of the user, frequently-used commands are built into command blocks.

Inputs to the model are: steer angles from the driver and steering control laws; drive/brake torques from the motors and brakes; and road input on running. The motor torque block can select an engine or motor module, from which the power source of the vehicle can be a combustion engine or electric motor. The vehicle dynamics block consists of the longitudinal, lateral, vertical, rolling, pitching, and yawing sub-blocks. The Dugoff tire model block produces tractive/braking and side forces at each wheel. Outputs from the model produce the state variables such as the vehicle velocity, yaw rate, sideslip angle, etc.

5. Simulation Results

The considered vehicle is 5 tons, similar to medium-duty trucks, and is driven by six 30hp AC motors with a gear ratio of 5:1. The motor torque is assumed constant in the 0~2400 rpm range and inversely proportional to the motor speed over 2400 rpm.

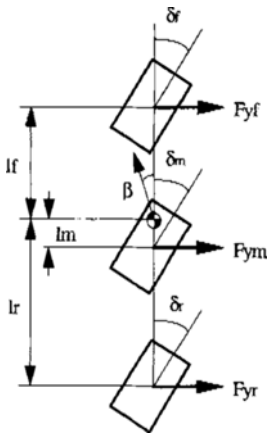

Fig. 6 2 DOF vehicle model

In order to investigate the coordination between the six wheels of the 6WS vehicle, 5 different steering modes are considered as shown in Fig. 5. For simplicity of comparison, the middle and the rear wheel steer angles are chosen form 0° or ±2°, and the front wheel steer angle is fixed to 4(in this section. However, in the next section, a new six wheel steering control law is proposed and its cornering performance is evaluated.

Frequency Response Analysis - Based on the 2 DOF linear model in Fig. 6, a frequency response analysis is carried out for comparing the five steering modes in Fig. 5. Assuming a constant speed of 80 km/h, the lateral acceleration and the yaw rate responses are compared in Fig. 7 and Fig. 8, respectively.

The lateral acceleration and the yaw rate frequency responses show the characteristics of a low-pass filter. That is, as the frequency of the steering input is increased, the response gain is decreased with increased phase lag. The lateral acceleration response shows that the gains of the 6WS vehicles are larger than the others but the phase lag of the 4WS vehicle is the smallest. The yaw rate response shows that the gains of the 6WS vehicles are the largest and the phase lag of the 6WS3 is the smallest. According to this analysis, it can be concluded that 6WS3, the coordinate mode of 6WS, is the best choice with fast yawing motion but at a cost of large lateral acceleration.

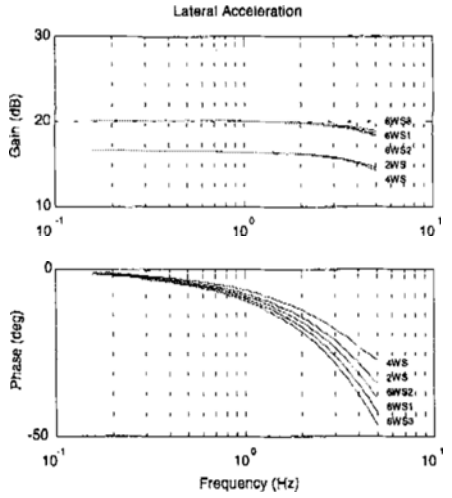

Fig. 7 Lateral acceleration frequency response

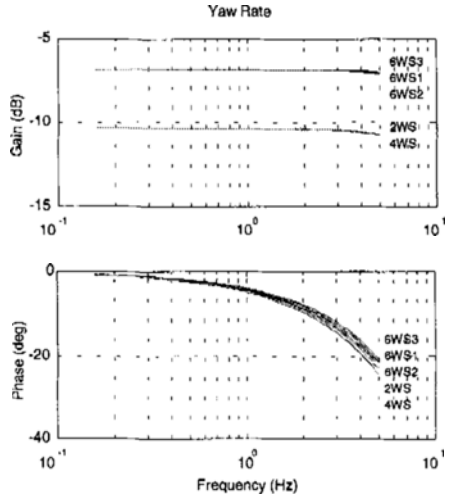

Fig. 8 Yaw rate frequency response

Because the linear model used here assumes that the mass center is located slightly forward from the vehicle center, the effect of rear wheel steering is large compared to that of middle wheel steering. However, in the next section the 18 DOF model will clearly show the effect of middle wheel steering.

Braking Steering - Braking while steering is a very common maneuver and its cornering performance is investigated based on the 18 DOF vehicle model introduced in the vehicle model section. While the vehicle is driving at 72 km/h, the brake

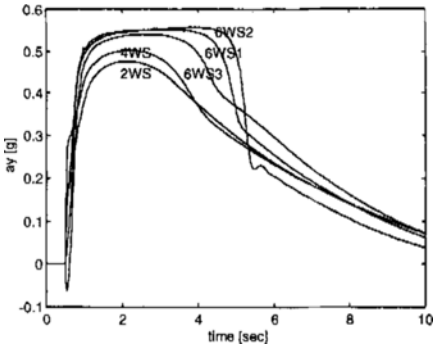

Fig. 9 Lateral acceleration

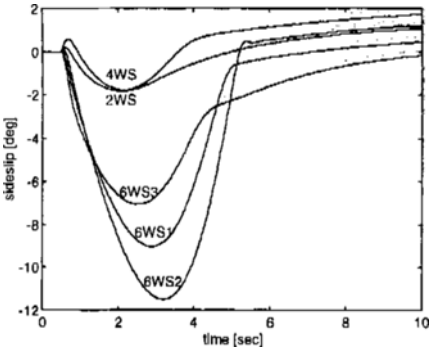

Fig. 11 Sideslip angle

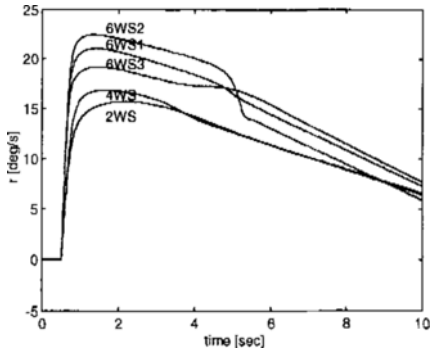

Fig. 10 Yaw rate

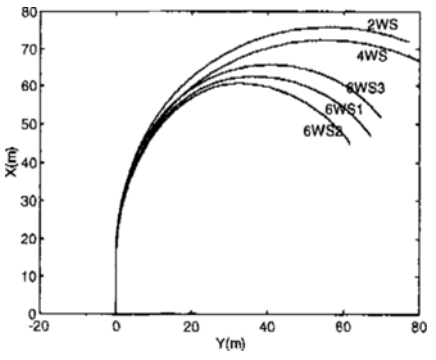

Fig. 12 Trajectory

torque is applied at each wheel and the steering is started from 0.5 second. The steer angle is increased and fixed into each steering mode listed in Fig. 5. Because the road condition is assumed unpaved, the friction coefficient is set to a value of 0.6.

Simulation results for the five steering modes in Fig. 5 are compared with respect to the lateral acceleration (Fig. 9), yaw rate (Fig. 10), sideslip angle (Fig. 11) and trajectory (Fig. 12). In general, 6WS modes have larger lateral acceleration, yaw rate, sideslip angle and smaller turning radius than 2WS and 4WS modes. Among 6WS modes, 6WS2 (crab-mode middle-wheel steering) gives the smallest turning radius with a large sideslip angle. This cornering difference, in particular the influence of the middle wheel steering, is caused by the nonlinear tire model and the weight transfer in the vehicle model.

Pivoting Pivoting is considered one of the special specifications of 6WD/6WS vehicles, and its feasibility is investigated in this section. Because electric motors are used for traction and steering, the direction and orientation of the motors are assumed to be easily changed for pivoting purposes. In order to pivot with respect to the geometrical center of the vehicle, the direction and the steer angle of the wheels should be in the form of Fig. 13. The driving torques applied to the middle wheels are smaller than the front/rear for geometrical equilibrium. The driving torque and the braking torque are selected such that the vehicle can stop after pivoting 180 degrees. The pivoting trajectory and the yaw angle response are plotted in Fig. 14 and Fig. 15, respectively, and demonstrate the feasibility of pivoting similar to tracked vehicles.

6. A Proposed 6WS Control Law

A new 6WS control law is proposed in order to minimize the sideslip angle during lane change

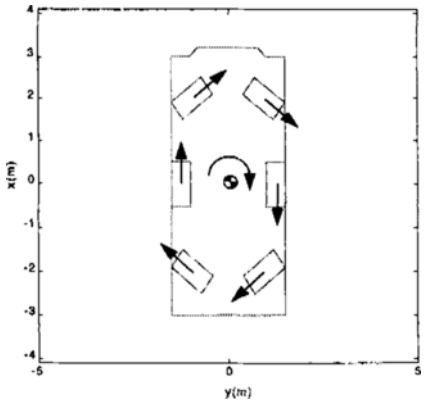

Fig. 13 Initial state

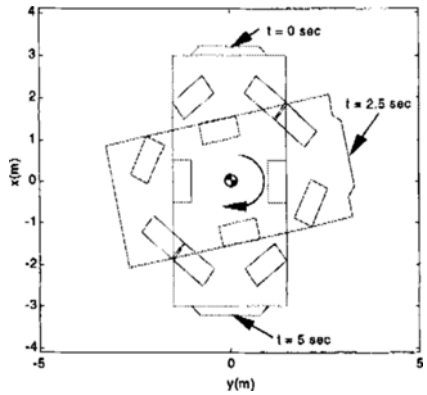

Fig. 14 Trajectory

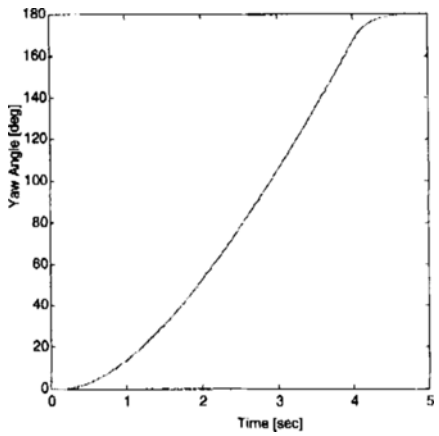

Fig. 15 Yaw angle

maneuvers. As illustrated in Fig. 9 and Fig. 11, 6WS vehicles with fixed steer angle have larger lateral acceleration and sideslip angle than 2WS and 4WS vehicles. This phenomena implies less maneuverability and less stability. To overcome this limitation, a new steering control law is developed based on the vehicle speed and the front wheel steer angle.

Vehicle Model - The vehicle model used for the controller design is a linear bicycle model having 2 DOF. Based on the bicycle model in Fig. 6, the equations of motion are derived taking into account the sideslip and the yaw rate.

lateral motion: $MV_x(\dot{\beta}+r)=2F_{yf}+2F_{ym}+2F_{yr}$ (14)

yawing motion: $I_z\dot{r}=2l_fF_{yf}-2l_mF_{ym}-2l_rF_{yr}$ (15)

where β is the sideslip angle, r is the yaw rate, Vx is the vehicle speed and other variables are explained in the nomenclature. Assuming that steer angles are small, the above equations can be rewritten into the following matrix form :

$$\begin{bmatrix}\dot{\beta}\\ \dot{r}\end{bmatrix}=\begin{bmatrix}-\frac{2}{MV_x}(C_f+C_m+C_r) & -1-\frac{2}{MV_x^2}(l_fC_f-l_mC_m-l_rC_r)\\ -\frac{2}{I_z}(l_fC_f-l_mC_m-l_rC_r) & -\frac{2}{I_zV_x}(l_f^2C_f+l_m^2C_m+l_r^2C_r)\end{bmatrix}\begin{bmatrix}\beta\\ r\end{bmatrix}+\begin{bmatrix}\frac{2C_f}{MV_x} & \frac{2C_m}{MV_x} & \frac{2C_r}{MV_x}\\ \frac{2l_fC_f}{I_z} & -\frac{2l_mC_m}{I_z} & -\frac{2l_rC_r}{I_z}\end{bmatrix}\begin{bmatrix}\delta_f\\ \delta_m\\ \delta_r\end{bmatrix} \quad (16)$$

Control Law - For a given vehicle speed and front wheel steer angle, the middle and the rear wheels need to steered appropriately for the required maneuvering and stability. In this section, assuming that the middle-wheel steer angle is half of the front steer angle, a steering control law for the rear wheels is developed to minimize the sideslip angle at the mass center. Similar to the 4WS case[3 and 4], the rear wheel steer angle is assumed to depend on the vehicle speed and the front steer angle.

$$\delta_m=\frac{1}{2}\delta_f \quad (17)$$

$$\delta_r=k_1\cdot\delta_f+k_2\cdot r \quad (18)$$

By substituting Eq. 17 and 18 into Eq. 16 and

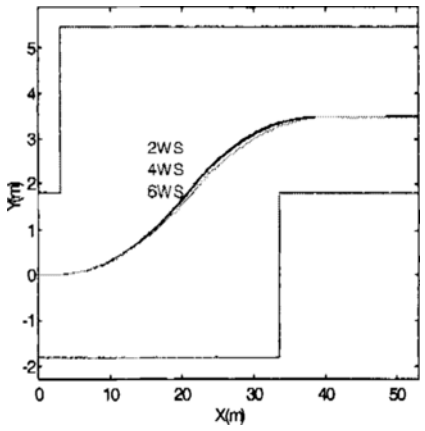

Fig. 16 Lane change trajectory

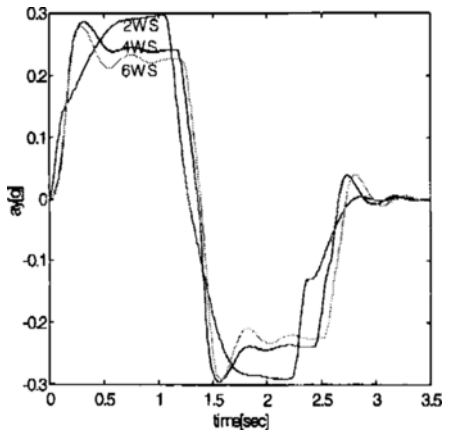

Fig. 18 Lateral acceleration

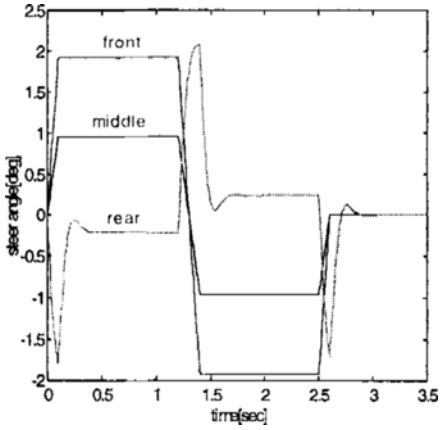

Fig. 17 6WS steer angle

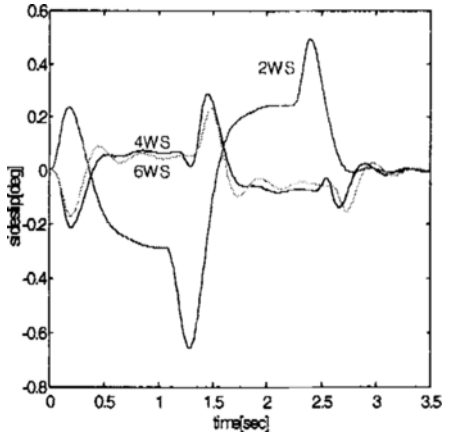

Fig. 19 Sideslip angle

setting to zero the determinant of the numerator of the transfer function between δ_f and β, the following relations are obtained for k1 and k2:

$$k_1 = -\frac{2C_f - C_m}{2C_r} \tag{19}$$

$$k_2 = \frac{MV_x^2 + 2(C_f l_f - C_m l_m - C_r l_r)}{2C_r V_x} \tag{20}$$

Lane Change - In order to evaluate the above control law compared to 2WS and 4WS, a lane change maneuver is simulated as shown in Fig. 16. The vehicle is supposed to follow the trajectory while maintaining a vehicle speed of 56 km/h. It is assumed that the front wheel is steered appropriately by a driver. In applying existing 4WS algorithms to the 6-wheeled vehicle, the middle wheel is not steered and the rear wheel is steered according to the algorithm. In the 6WS case, the middle wheel is steered to half of the front wheel steering angle and the rear wheel is steered according to the proposed control law as shown in Fig. 17.

$$\text{4WS law: } \delta_r = -\frac{C_f + C_m}{C_r}\delta_f + \frac{MV_x^2 + 2(C_f l_f - C_r l_r)}{2C_r V_x} r \tag{21}$$

$$\text{6WS law: } \delta_r = \frac{-2C_f - C_m}{2C_r}\delta_f + \frac{MV_x^2 + 2(C_f l_f - C_m l_m - C_r l_r)}{2C_r V_x} r \tag{22}$$

where C_f, C_m, and Cr are the cornering stiffness of the front, middle and rear wheels, respectively.

Lane change results show that the proposed 6WS control law follows the desired trajectory with less steer angles than 2WS and 4WS. The

lateral acceleration (Fig. 18) in the 6WS case is slightly smaller than the 2WS and 4WS cases, but the sideslip angle (Fig. 19) in the 6WS case is much smaller than the 2WS case and smaller than the 4WS case.

7. Conclusions

A Frequency analysis based on a 2 DOF linear model shows that 6WS vehicles have larger gain in lateral acceleration and yaw rate than 2WS and 4WS vehicles. In order to analyze the cornering performance of 6WD/6WS vehicles, an 18 DOF nonlinear vehicle model is developed and constructed into a simulation tool using MATLAB/SIMULINK. Simulation results for cornering combined with braking demonstrate the role of middle wheel steering in 6WS vehicles. In particular, when the middle wheel is in the same direction as the front wheel (crab mode), the turning radius can be reduced with increased sideslip angle. To overcome this limitation, a new 6WS control law is proposed to minimize the sideslip angle. Lane change maneuvering results indicate improved stability and maneuverability of 6-wheeled vehicles. A feasibility study for the pivoting of 6-wheeled vehicles is completed and illustrates the unique characteristics of electric-driven multi-wheeled vehicles.

References

Abe, M., 1989, "Handling Characteristics of Four Wheel Active Steering Vehicles over Full Maneuvering Range of Lateral and Longitudinal Accelerations," *Proceedings of 11th IAVSD Symposium, Vehicle System Dynamics*, Vol. 18 pp. 1~14.

Allen, R. W., Rosenthal, T. J. and Szostak, H. T., 1987, "Steady State and Transient Analysis of Ground Vehicle Handling," *SAE* 870495.

Bakker, E., Pacejka, H. B. and Lidner, L., 1989, "A New Tire Model with an Application in Vehicle Dynamics Studies," *SAE* 890087.

Das, N. S., Suresh, B. A. and Wambold, J. C., 1993, "Estimation of Dynamic Rollover Threshold of Commercial Vehicles Using Low Speed Experimental Data," *SAE* 932949.

Dugoff, H., Fancher, P. S. and Segel, L., 1970, "An Analysis of Tire Traction Properties and Their Influence on Vehicle Dynamic Performance," *SAE Transactions*, 79:341-366, SAE Paper No. 700377.

Hata, N., Osanai, H., Hasegawa, S., Takahashi, S. and Watanabe, Y., 1992, "An Investigation into Vehicle Controllability and Stability of an Experimental Medium-Duty Truck with Rear-Axle Steering," *AVEC* 923044.

Metz, L. D., 1993, "Dynamics of Four-Wheel-Steer Off-Highway Vehicles," *SAE* 930765.

Nalecz, A. G. and Bindermann, A. C., 1988, "Investigation into the Stability of Four Wheel Steering Vehicles," *Int. J. of Vehicle Design*, Vol. 9, No. 2, pp. 159~178.

Nasu, H. and Higasa, H., 1995, "Development of Yonden Electric Vehicle PIVOT," *JSAE*, Review 16, pp. 77~82.

Ogorkiewicz, R. M., 1968, *Design and Development of Fighting Vehicles*, Macdonald and Co (publishers) Limited, pp. 172~193.

Pillar, D. R. and Braun, E. E., 1995, "All-Wheel Steering System for Heavy Truck Application," *SAE* 952680.

Smith, D. E. and Starkey, J. M., 1995, "Effects of Model Complexity on the Performance of Automated Vehicle Steering Controllers : Model Development, Validation and Comparison," *Vehicle System Dynamics*, Vol. 24, pp. 163~181.

Xia, X. and Law, E. H., 1992, "Nonlinear Analysis of Close-Loop Driver/Automobile Performance with Four Wheel Steering Control," *SAE* 92055.

Jang, J. H. and Han, C. S., 1997, "Sensitivity Analysis of Side Slip Angle for a Front Wheel Steering Vehicle : a Frequency Domain Approach," *KSME International Journal*, Vol. 11, No. 4, pp. 367~378.

Jang, J. H. and Han, C. S., 1997, "The State Sensitivity Analysis of the Front Wheel Steering Vehicle : In the Time Domain," *KSME International Journal*, Vol. 11, No. 6, pp. 595~604.